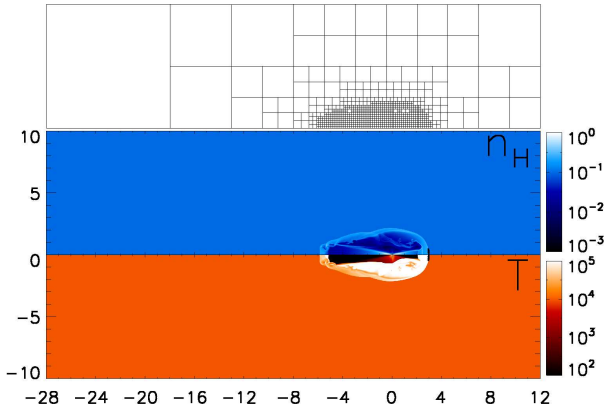

Fig. 3. Density (color scale given in cm^{-3}, middle panel) and temperature (color scale given in K, bottom panel) stratifications. The corresponding mesh configurations (on top of each density/temperature plot) are also shown, with each square representing a 24×24 grid point block. The results are for model 1 at $t = 1 \times 10^3$ yr. The axes are labeled in units of 10^{17} cm (the figure only shows the inner half of the radial extent, the rest is unperturbed). The color figure can be viewed online.

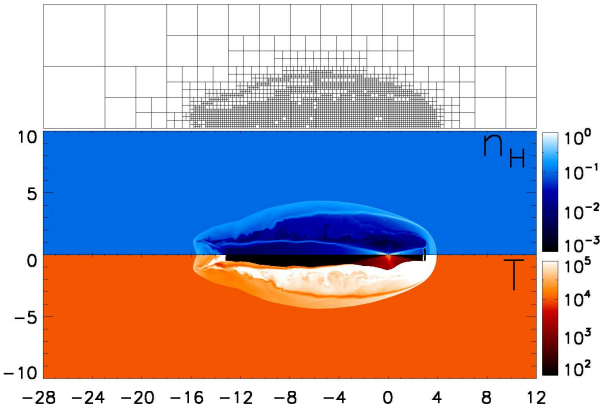

Fig. 4. Same as Figure 3 at $t = 3 \times 10^3$ yr. The color figure can be viewed online.

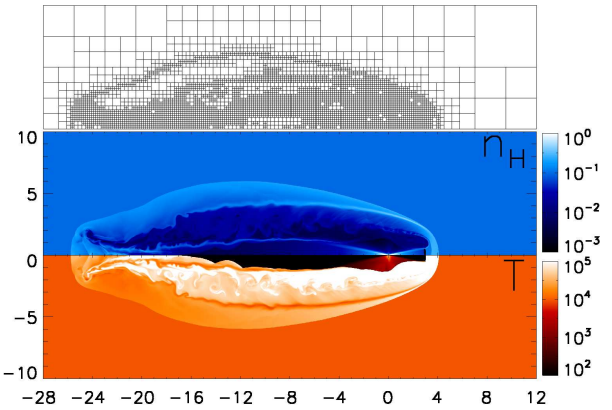

Fig. 5. Same as Figure 3 at $t = 5 \times 10^3$ yr. The color figure can be viewed online.

In Table 1 we have also included the corresponding value of the bow-shock standoff distance R_0 (see equation 10), and the cooling distances associated with the double shock structure at R_0. The cooling distance ${d_c}^f$ corresponds to the forward shock (with the streaming ambient medium), while ${d_c}^r$ corresponds to the cooling behind the reverse shock. In order to calculate these cooling distances, we have used the fit:

$$ {d_c}^i = \left(\frac{100\,\mathrm{cm}^{-3}}{n_0^i}\right)\left\{\left[3\times10^{11}\mathrm{cm}\right]\left(\frac{u_0^i}{100\,\mathrm{km\,s}^{-1}}\right)^{-6.4} + \left[8\times10^{13}\mathrm{cm}\right]\left(\frac{u_0^i}{100\,\mathrm{km\,s}^{-1}}\right)^{5.5}\right\}, \quad (11) $$

to the cooling distances to 10^4 K given in the tabulation of self-consistent preionization, plane-parallel shock models of Hartigan, Raymond, & Hartmann (1987). In equation (11), n_0 is the pre-shock atom+ion number density, and u_0 is the shock velocity.

4. RESULTS

In Figures 3–5, we show the time-evolution ($t = 1\times10^3$, 3×10^3, and 5×10^3 yr, respectively) obtained from model 1 (see Table 1). For each time, we show the corresponding mesh configuration, the density n_H (in cm^{-3}) and the temperature T (in K) (top, middle, and bottom panels, respectively). Thanks to the adaptive grid of the code we used less than 10% (for $t \times 10^3$ yr) and 20% (for $t > 10^3$ yr) of the finest grid in the domain, thus notably reducing the required computer time.

From the time-sequence shown in Figures 3–5, we see that the flow develops a cometary-shaped structure, due to the presence of the side-streaming environmental wind (which flows parallel to the z-axis, from right to left). The head of the cometary structure approaches the steady state star/bow shock stagnation distance R_0 (see § 2) at a time $t \approx 10^3$ yr.

In Figure 6, we show single time frames ($t = 5 \times 10^3$ yr) of the density and temperature stratifications (top and bottom parts, respectively, of each of the three panels) obtained from models 1 through 3 (see Table 1). In each plot we include the corresponding "thin shell" analytic solution (see § 2).

Even though models 1 through 3 differ in $\dot{M}_j$ and Θ (see Table 1), they result in basically the same flow morphology. Model 3 (which has the largest